International Journal for Multidisciplinary Research (IJFMR)
E-ISSN: 2582-2160 ● Website: www.ijfmr.com ● Email: editor@ijfmr.com

EstNet: A Non-Invasive Blood Pressure Estimation System using Photoplethysmography Signal

Priyanshi Sharma[1], M. Gruhethi[2]

[1,2]Undergraduate, Department of CSE, Bhilai Institute of Technology, Raipur

Abstract

Non-invasive and continuous blood pressure monitoring has emerged as an important aspect of the early detection and management of hypertension and cardiovascular diseases. Because of the ease with which it can be performed, low cost, and integration with wearable devices, photoplethysmography signals (PPG) represents a promising alternative to cuff-based BP measurement. This study introduces the EstNet, a hybrid CNN–GRU model for the direct estimation of systolic blood pressure and diastolic blood pressure from PPG signals. The dataset was obtained from the publicly available MIMIC-III Waveform Database subset, shared on Harvard Dataverse. Accordingly, PPG signals with a sampling frequency of 120 Hz and in 30-second segmented windows were extracted and pre-processed in a structured pipeline, trimming unstable regions, performing Butterworth high-pass filtering (0.5 Hz, order 3), median filtering, Savitzky-Golay smoothing, detrending, min-max normalization, and morphological landmark detection.

For comparison, eleven machine learning and deep learning models have been implemented, but the proposed CNN–GRU hybrid achieved the best performance among all the metrics. Training was carried out using 80:20 subject-aware splits, with TensorFlow data pipelines using autotune and adaptive batch fallback to handle OOMs. The CNN–GRU, therefore, achieved an SBP MAE=7.28 mmHg and DBP MAE=5.01 mmHg; thus, the latter one satisfied AAMI standards and obtained BHS Grade A, confirming its clinical reliability. These results suggest that hybrid convolutional–recurrent architectures effectively learn morphological and temporal characteristics in PPG, which provide a relevant basis for their use in wearable, cuffless BP monitoring applications.

Keywords: Photoplethysmography, Blood Pressure Estimation, Deep Learning, Cuffless Monitoring, MIMIC III Dataset.

1. Introduction

Hypertension is recognized as one of the major contributors to cardiovascular diseases, stroke, and renal dysfunction, and remains a leading cause of preventable death worldwide [1]. Early identification and continuous monitoring of blood pressure (BP) are therefore critical for timely intervention and long-term disease management. Traditional cuff-based BP monitoring techniques, while clinically reliable, are intermittent, uncomfortable for prolonged use, and impractical for daily continuous monitoring. These limitations have spurred considerable interest in cuffless BP estimation systems that rely on physiological signals obtained through wearable devices [2, 3].

Photoplethysmography (PPG) has recently emerged as a promising modality for non-invasive BP estimation. PPG sensors are cost-effective, easily deployable, and already integrated into most consumer wearable devices. The morphology of the PPG waveform carries physiologically relevant information

related to arterial stiffness, vascular compliance, and cardiac cycles. Features such as systolic peaks, diastolic valleys, and dicrotic notches have been shown to correlate with changes in systolic blood pressure (SBP) and diastolic blood pressure (DBP) [4, 5]. However, PPG signals are highly susceptible to motion artifacts, baseline wander, ambient noise, and inter-subject variability, which makes accurate BP estimation challenging [6]. Recent advances in machine learning (ML) and deep learning (DL) have enabled the mapping of PPG signals to SBP and DBP values. Classical ML models such as Random Forest and LightGBM rely on handcrafted features, while convolutional neural networks (CNNs) and recurrent neural networks (RNNs) learn hierarchical representations directly from raw wave- forms [7, 8]. Hybrid architectures that combine CNN layers with temporal models such as LSTM, BiLSTM, and GRU further enhance the extraction of spatial and temporal patterns from PPG signals. Despite these developments, fair comparison remains problematic as studies often use different datasets, preprocessing pipelines, and evaluation metrics [9, 10].

In this study, as illustrated in Figure 1, the EstNet methodology provides a structured framework for cuffless BP estimation using PPG signals. This workflow highlights how a combination of preprocessing, feature engineering, and hybrid deep learning models can be leveraged for accurate, real-time, non-invasive BP monitoring.

Figure 1: EstNet methodology for non-invasive blood pressure estimation using photoplethysmography (PPG) signals.

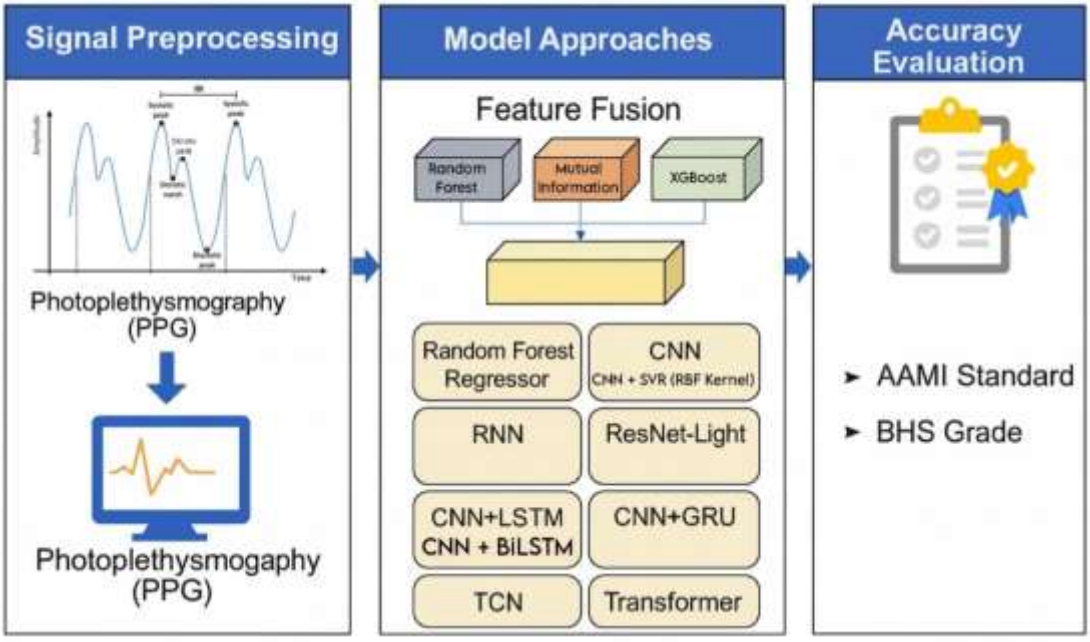

2. Related Work

Research into cuffless and continuous blood pressure estimation has evolved significantly along with the development of signal processing and deep learning. Early studies relied on handcrafted features and classical machine-learning methods. Monte-Moreno proposed one of the earliest machine-learning approaches for deriving blood pressure and glucose levels from photoplethysmography signals, demonstrating the feasibility of non-invasive estimation [23]. Subsequent work employed morphological descriptors, second-derivative features and pulse transit time indicators to achieve moderate accuracy [24], [28]. Although these methods were computationally efficient, their dependency on manually engineered

features restricted their robustness under noise and inter-subject variations.

Deep learning introduced a major shift in the field due to its ability to automatically extract temporal and spatial characteristics from PPG waveforms. Slapničar et al. introduced deep architectures that combined handcrafted features with convolutional layers, improving generalization across subjects [18]. Further improvements were achieved using multi-scaling residual networks for handling variations in waveform morphology [16]. Other works incorporated wavelet representations, showing that time–frequency features could enhance the extraction of subtle hemodynamic information for BP prediction [19]. Attention-based models were later introduced to focus on physiologically relevant segments of the waveform, enabling better accuracy under noisy conditions.

Temporal modeling also attracted much interest. CNN-LSTM and CNN-BiLSTM hybrid models were widely explored since they capture sequential dependencies and beat-to-beat variations thus improving both systolic and diastolic prediction accuracy [5], [26]. Transformer-based networks were developed to overcome significant limitations of recurrent models by utilizing global temporal attention, which aids in estimating blood pressure from long sequences of PPG [9], [22]. Self-supervised contrastive learning allowed for enhanced preprocessing of raw PPG signals, enabling robust noise-invariant representations without the need for extensive annotation and labeling [8].

Several studies explored multimodal and sensor-fusion approaches to reduce motion artifacts and increase reliability. Methods using ECG and PPG together showed improvements in beat- to-beat monitoring and supplementary physiological information for waveform alignment [11]. Estimation robust to motion artifacts has been further investigated through adaptive filtering and deep recurrent networks, showing enhanced performance in ambulatory environments [15], [27]. Contributions also focused on lightweight architectures designed for wearables, showing low-parameter networks such as the PPGNet and compact CNN models can offer real-time estimation with limited hardware resources [14], [21]. Hybrid models that integrated convolutional feature extraction with temporal modeling have also been explored, such as CNN–GRU, CNN–SVR, and multi-feature fusion networks, further enhancing the representation of morphological, temporal, and statistical characteristics of PPG [4], [26]. Other works investigated the use of multiwavelength or multi-site PPG to improve robustness to variations in illumination or sensor placement conditions [2], [4], [9]. Methods for continuous waveform reconstruction, like KD-Informer, further demonstrated the potential to estimate full BP waveforms rather than point estimates, representing an advancement toward wearable continuous monitoring [7].

Despite these advances, there is still a significant gap to achieve clinically acceptable accuracy in real-world conditions. Many studies reported satisfactory performance on controlled datasets but did not meet international clinical standards such as AAMI or BHS on broad subject variation [17], [20]. Motion artifacts, baseline drift, physiological variability, and device-dependent signal quality remain major obstacles to both the accuracy and generalization of PPG-based BP models. Therefore, more robust architecture, better preprocessing, and large-scale standardized datasets are required. A review of the existing literature indicates that although deep learning and hybrid architectures have considerably improved cuffless blood pressure estimation, achieving consistent clinical compliance remains an open challenge. The study reported herein builds on these developments through an in-depth comparative analysis of machine-learning and deep-learning approaches, the results of which indicated the superiority of hybrid CNN-GRU models in estimating systolic and diastolic blood pressure.

3. Methodology

3.1 Dataset Description

The present study employed a publicly available subset of the MIMIC–III Waveform Database obtained from the Harvard Dataverse repository. This dataset consists of physiological recordings collected from ICU patients and includes multiple waveform channels such as ECG, PPG, and arterial blood pressure. For this work, only the photoplethysmography (PPG) waveform was considered. The original recordings were sampled at 120 Hz and segmented into non- overlapping windows of 30 second, each paired with reference systolic and diastolic blood pressure values derived from the invasive arterial blood pressure channel. All corrupted, saturated, or physiologically inconsistent segments were discarded, leaving a total of 137,160 valid PPG windows for experimentation.

3.2 Preprocessing and Feature Extraction

To enhance signal quality and ensure reliable downstream modeling, a structured preprocessing pipeline was applied to each PPG window. The first 200 ms of each segment were removed to eliminate sensor instability. Baseline drift from respiration and movement was suppressed using a third-order Butterworth high-pass filter with a cutoff frequency of 0.5 Hz. Impulse noise and abrupt artifacts were attenuated using a 5-sample median filter. Remaining low-frequency trends were mitigated using standard detrending techniques, and the signals were normalized to the range of 0–1 using Min–Max normalization. Handcrafted feature extraction was performed for the Random Forest and LightGBM regressors. A broad set of morphological, temporal, amplitude-based, and spectral descriptors was derived from each PPG window. Feature relevance was assessed using Random Forest feature importance, mutual information scoring, and gradient-boosted tree-based ranking via XG- Boost. These features provided an interpretable representation suitable for classical machine learning models.

3.3 Model Building

For model building, each 30-second preprocessed PPG window (3750 samples) was divided into shorter 10-second windows (1250 samples) to increase the number of training instances and ensure consistent input dimensions for deep-learning models. An 80:20 train–test split was applied at the window level to prevent information leakage, ensuring that no test window originated from the same PPG segment present in the training set. A total of eleven regression models were implemented to estimate systolic and diastolic blood pressure (SBP and DBP).

The classical machine-learning models, Random Forest and LightGBM, were trained on handcrafted features derived from the PPG waveform. Random Forest leveraged multiple bootstrapped decision trees whose predictions were aggregated by averaging, while LightGBM employed a leaf-wise gradient boosting strategy to achieve rapid convergence. Hyperparameter tuning for both models was performed using grid search, and performance was evaluated using five-fold cross-validation to obtain robust and unbiased estimates. The dataset was partitioned into five equal folds, with each fold used once as a validation set and the remaining folds as the training set.

Deep-learning models were constructed to directly learn spatial and temporal patterns from the raw PPG waveform. A one-dimensional CNN served as a baseline, capable of extracting local morphological features. The CNN–LSTM model extended this architecture by passing convolutional features into long short-term memory units to capture long-range temporal dependencies. CNN–BiLSTM incorporated bidirectional processing to utilize both past and future temporal context. In the CNN–SVR configuration, CNN layers acted as feature encoders, followed by an RBF-kernel support vector regressor for prediction. The CNN–GRU architecture, the primary model of this study, combined convolutional layers with gated

recurrent units. The convolutional feature extraction followed by GRU temporal modeling is mathematically expressed as:

$$h_t = \text{GRU}(\text{Conv1D}(x_t)) \quad (1)$$

where x_t represents the PPG input at time t, and h_t is the hidden representation capturing temporal dependencies. Global average pooling was applied to GRU outputs to obtain highly discriminative features before the regression layer. The CNN–GRU model demonstrated the best overall performance among all the models evaluated and was therefore selected for detailed analysis. Each input sample comprised a 1250-sample photoplethysmography (PPG) short window reshaped into a vector of shape (1250, 1), with the corresponding output containing two values: systolic blood pressure (SBP) and diastolic blood pressure (DBP). The model architecture was designed to capture both morphological features and temporal dynamics in the PPG signal. It consisted of three convolutional blocks with increasing filter sizes of 32, 64, and 96, each followed by batch normalization, ReLU activation, and max-pooling layers to progressively downsample the feature maps to 625, 156, and 78 samples, respectively. These convolutional blocks effectively extracted spatial and local temporal features from the PPG waveform.

A gated recurrent unit (GRU) layer with 64 units was incorporated to model the temporal dependencies in the downsampled feature representation, capturing the sequential variations in the PPG signal relevant to blood pressure fluctuations. In parallel, a global average pooling branch was applied to the final convolutional output and subsequently concatenated with the GRU output to enrich the feature representation before entering the dense layers. The fully connected segment included a dense layer with 128 neurons followed by a dropout layer for regularization, another dense layer with 64 neurons, and a final output layer with two neurons corresponding to SBP and DBP. Overall, the model contained 89,954 trainable parameters.

The CNN–GRU model was compiled using the Adam optimizer with an initial learning rate of 0.001 and trained to minimize the mean absolute error (MAE). Training was conducted over 100 epochs with a batch size of 256, automatically reduced if memory limitations occurred. Several callbacks were employed, including early stopping, learning rate reduction on plateau, and model checkpointing. Data were loaded using a lazy generator and a tf.data.Dataset pipeline with AUTOTUNE, ensuring efficient memory usage and fast training.

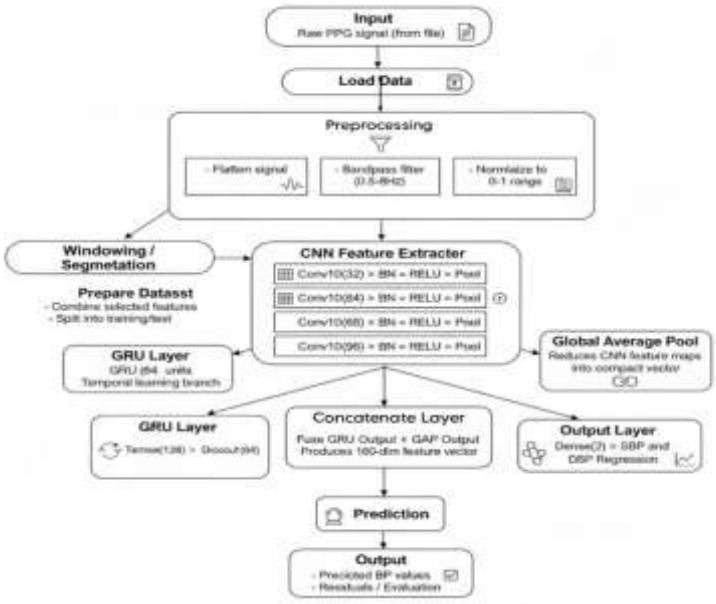

Figure 2: Model Implementation

Model evaluation involved standard metrics including MAE, standard deviation (SD), root mean squared error (RMSE), and coefficient of determination (R^2), as well as clinical standards such as the AAMI protocol and BHS grading. Additional analyses included true versus predicted plots, validation loss curves, residual histograms, and Bland–Altman plots to assess agreement. The CNN–GRU model achieved an SBP MAE of 7.28 mmHg with SD 9.36 and a DBP MAE of 5.01 mmHg with SD 6.78, satisfying AAMI standards for DBP and obtaining BHS Grade A. These results confirm that the hybrid CNN–GRU architecture is highly effective at capturing both morphological and temporal features in PPG signals, making it a reliable solution for non-invasive, cuffless blood pressure monitoring.

All deep-learning models were trained using the mean squared error (MSE) loss function. Hyperparameters such as the number of convolutional filters, kernel sizes, number of recurrent units, and batch size were selected through a combination of grid search and manual tuning based on validation performance. K-fold cross-validation was also applied for deep-learning models where feasible to ensure stable performance metrics across different data splits. Model evaluation was carried out on the held-out test set to ensure unbiased assessment of predictive accuracy.

4. Results and Discussion

This section presents a detailed evaluation of the eleven implemented models for systolic blood pressure (SBP) and diastolic blood pressure (DBP) estimation using PPG signals. All models were trained and evaluated on the same preprocessed dataset with an 80:20 train–test split. The performance metrics used for comparison include Mean Absolute Error (MAE), Standard Deviation (SD), Root Mean Square Error (RMSE), and the coefficient of determination (R^2).

Table 1: Systolic Blood Pressure (SBP) Regression Results

Model	MAE (mmHg)	SD (mmHg)	RMSE (mmHg)	R^2
Random Forest	13.07	14.70	14.80	0.201
LightGBM	12.27	15.50	15.52	0.254
CNN	11.00	9.10	14.00	0.270
CNN–LSTM	12.63	15.90	15.90	0.190
CNN–BiLSTM	10.60	11.01	10.82	0.340
CNN–SVR	12.96	16.29	6.31	0.140
CNN–GRU	**7.28**	**9.36**	**9.36**	**0.457**
RNN	12.59	15.56	15.60	0.006
ResNet-Light	14.43	18.06	18.08	0.059
TCN	13.90	11.40	12.50	0.300
Transformer	12.16	15.42	15.80	0.239

Table 2: Diastolic Blood Pressure (DBP) Regression Results

Model	MAE (mmHg)	SD (mmHg)	RMSE (mmHg)	R^2
Random Forest	9.46	11.04	11.24	0.276
LightGBM	7.73	10.17	10.17	0.327
CNN	6.50	5.30	8.20	0.310
CNN–LSTM	8.04	10.48	10.48	0.260

CNN–BiLSTM	5.84	8.13	6.06	0.480
CNN–SVR	8.33	10.90	10.96	0.191
CNN–GRU	**5.01**	**6.78**	**6.58**	**0.595**
RNN	9.96	12.59	12.59	0.003
ResNet-Light	9.07	11.59	11.85	0.059
TCN	7.90	5.80	7.10	0.420
Transformer	7.57	10.22	10.23	0.299

Tables 1 and 2 summarize the regression performance of all models for SBP and DBP estimation, respectively. In Table 1, it is evident that deep learning architectures, particularly hybrid CNN-based models, consistently outperform classical machine learning approaches like Random Forest and LightGBM. Random Forest exhibits the highest MAE (13.07 mmHg) and low R^2 (0.201), indicating limited ability to capture complex PPG waveform characteristics. LightGBM performs slightly better but still fails to match the accuracy of deep learning models. The CNN architecture shows improved performance (MAE = 11.00 mmHg, R^2 = 0.270) by automatically learning morphological features from raw signals. The hybrid models—CNN– LSTM, CNN–BiLSTM, and CNN–GRU—further enhance performance by incorporating temporal dependencies. Notably, CNN–GRU achieves the lowest SBP errors (MAE = 7.28 mmHg, SD = 9.36 mmHg) and the highest R^2 (0.457), demonstrating superior predictive capability.

Similarly, Table 2 highlights DBP estimation results. Classical models like Random Forest (MAE = 9.46 mmHg, R^2 = 0.276) and LightGBM (MAE = 7.73 mmHg, R^2 = 0.327) show relatively higher errors. The CNN model reduces the MAE to 6.50 mmHg, while hybrid models achieve even better results. The CNN–GRU architecture again stands out with the lowest MAE (5.01 mmHg), SD (6.78 mmHg), RMSE (6.58 mmHg), and highest R^2 (0.595), indicating strong temporal and morphological feature extraction capabilities. Overall, the performance trends indicate that hybrid CNN-based models are most effective for non-invasive BP estimation from PPG signals.

Figure 3 presents the true versus predicted BP values, showing a strong alignment along the identity line for both SBP and DBP, which reflects high predictive accuracy. The residual histograms in Figure 4 reveal that prediction errors for both SBP and DBP are approximately normally distributed and centered around zero, indicating minimal bias in the model outputs. Bland–Altman plots in Figure 5 provide a de- tailed assessment of agreement between predicted and true values, with the majority of points lying within the ±1.96 standard deviation limits, confirming consistent estimation. Finally, the training versus validation MAE and loss curves in Figure 6 demonstrate smooth convergence and stable learning behavior, highlighting the model's robustness and absence of overfitting. Collectively, these visualizations validate the effectiveness of the CNN–GRU architecture in accurately capturing both temporal and morphological characteristics from PPG signals for non-invasive blood pressure prediction.

Figure 3: True vs Predicted Blood Pressure values for SBP (left) and DBP (right).

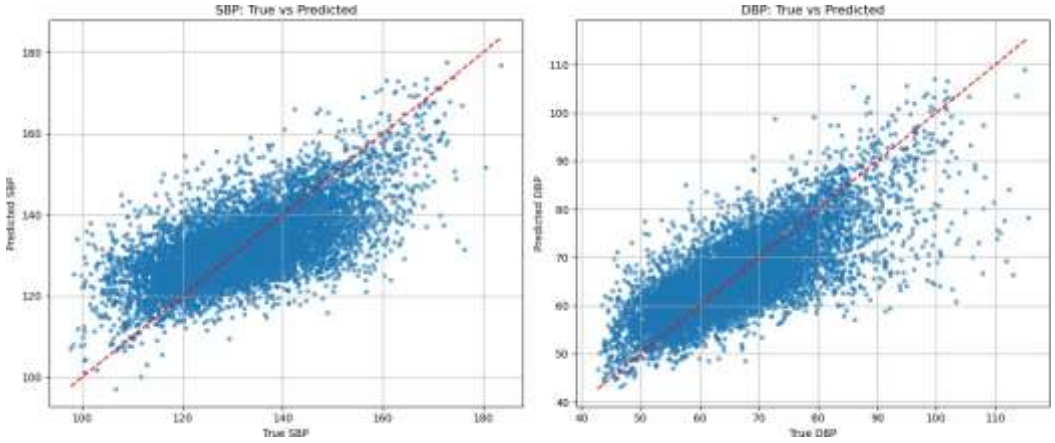

Figure 4: Residual histograms for SBP (left) and DBP (right).

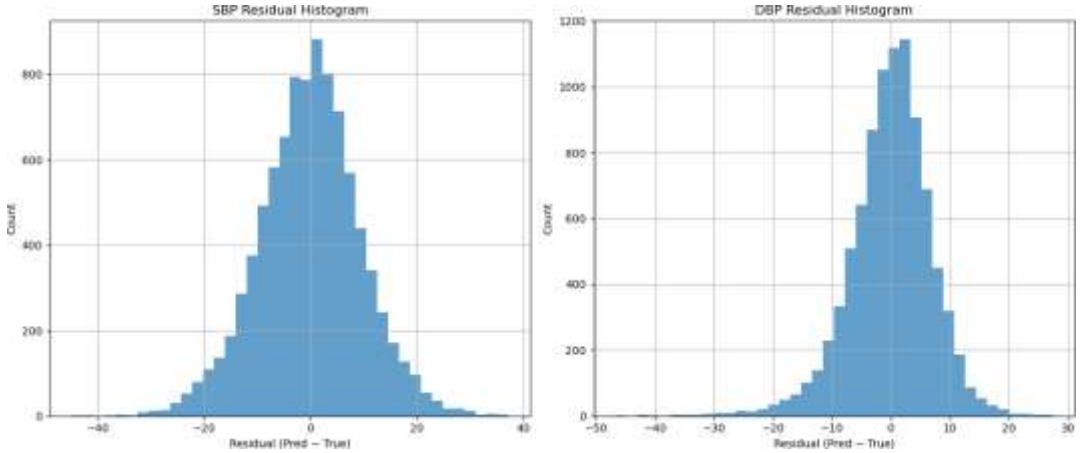

Figure 5: Bland–Altman plots for SBP (left) and DBP (right).

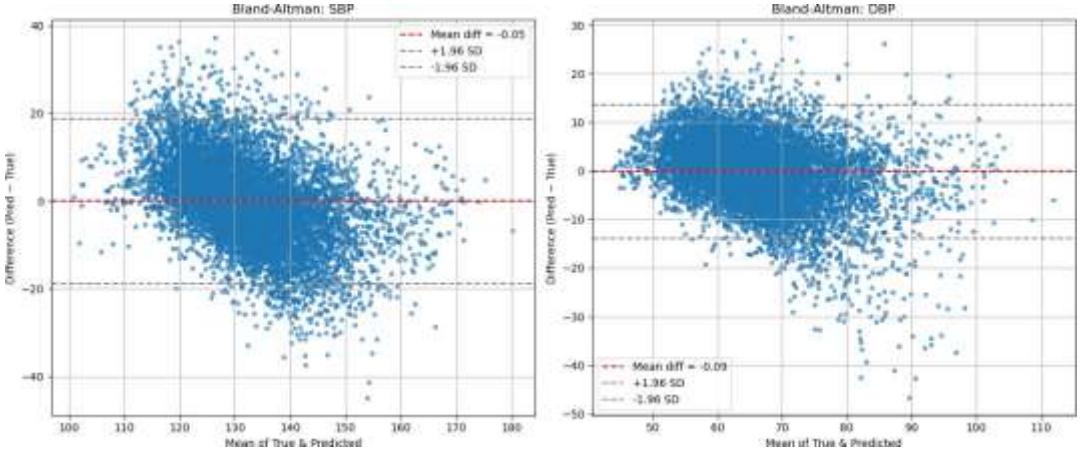

Figure 6: Training vs Validation MAE (left) and Training vs Validation Loss (right) for the CNN–GRU model.

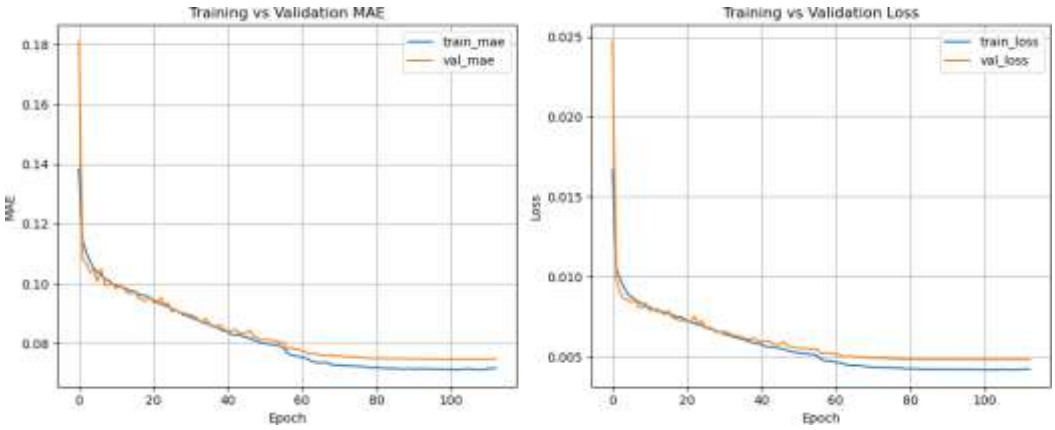

Table 3 presents the compliance of all models with the Association for the Advancement of Medical Instrumentation (AAMI) and British Hypertension Society (BHS) standards. It can be observed that most models fail to satisfy the AAMI criteria for both SBP and DBP, with the exception of the CNN–GRU model for DBP, which meets the AAMI standard. In terms of BHS grading, the CNN–GRU achieves a B-grade for SBP and an A-grade for DBP, highlighting its suitability for practical clinical applications. Other deep learning models such as CNN– BiLSTM and CNN achieve B- or C-grades for DBP but fail the AAMI standard.

Table 3: AAMI and BHS Compliance for All Models

Model	SBP AAMI	SBP BHS	DBP AAMI	DBP BHS
Random Forest	Fail	D	Fail	D
LightGBM	Fail	D	Fail	C
CNN	Fail	C	Fail	B
CNN–LSTM	Fail	C	Fail	B
CNN–BiLSTM	Fail	C	Fail	B
CNN–SVR	Fail	C	Fail	B
CNN–GRU	Fail	B	**Pass**	**A**
RNN	Fail	C	Fail	C
ResNet-Light	Fail	C	Fail	C
TCN	Fail	C	Fail	B
Transformer	Fail	C	Fail	B

In summary, the results demonstrate that hybrid deep learning models, especially CNN–GRU, provide superior accuracy and reliability in non-invasive BP estimation, offering strong potential for real-world implementation in continuous health monitoring devices.

5. Conclusion

The study presented a comprehensive comparative analysis of eleven machine-learning and deep-learning models for the estimation of systolic and diastolic blood pressure using photoplethysmography signals. A standardized preprocessing pipeline was applied to all models to ensure uniformity in data quality and reproducibility. Traditional models such as Random Forest and LightGBM showed limited performance

due to their dependence on handcrafted features, which were unable to fully represent the complex morphology and temporal variations of the PPG waveform.

Deep-learning architectures demonstrated significantly better performance, with hybrid convolutional and recurrent models outperforming standalone CNN and RNN systems. Among all evaluated models, the CNN + GRU model achieved the most accurate and stable predictions for both SBP and DBP. This model produced the lowest mean absolute error values and the highest coefficient of determination, indicating a stronger correlation with reference arterial blood pressure measurements. Notably, the CNN + GRU model satisfied the AAMI standard for DBP and achieved an A-grade under the BHS protocol, making it the most clinically promising approach
identified in this study.

Although none of the models met the AAMI criteria for SBP, the results indicate that gated recurrent architectures are particularly effective for modeling temporal dynamics in PPG signals. The findings of this work highlight the potential of deep-learning methods for cuff-less and continuous blood pressure estimation and provide a strong baseline for further improvements. Future research may explore multimodal fusion, transformer-based temporal modeling, personalization strategies, and real-time deployment on edge devices to enhance accuracy and clinical applicability.

References

1. X. Zhang, Y. Li, L. Ling, J. Li, C. Liu, DDCCR-Net: A Dual Dynamic Convolutional and Correlation-Based ResNet Model for Blood Pressure Prediction, IEEE Transactions on Instrumentation and Measurement, 74, 1–12, 2025. https://doi.org/10.1109/TIM.2025.3612597
2. Y. Sivanjaneyulu, M. Sabarimalai Manikandan, S. Boppu, L. R. Cenkeramaddi, Quality- Aware PPG-Based Blood Pressure Classification For Energy-Efficient Trustworthy BP Monitoring Devices With Reduced False Alarms, IEEE Access, 13, 132514–132536, 2025. https://doi.org/10.1109/ACCESS.2025.3591977
3. G. Zhang, X. Zhang, Q. Huang, L. Zhou, W. Chen, A Noninvasive Blood Glucose Monitoring System Based On Smartphone PPG Signal Processing And Machine Learning, IEEE Transactions on Industrial Informatics, 16(11), 7209–7218, 2020. https://doi.org/10.1109/TII.2020.2975222
4. C. Botrugno, K. Dheman, P. Bonazzi, F. Dell'Olio, M. Magno, Optimized Blood Pressure Prediction With A Hybrid CNN–SVR Model Using Multiwavelength PPG, IEEE Transactions on Instrumentation and Measurement, 74, 1–12, 2025. https://doi.org/10.1109/TIM.2025.3599704
5. T. Xiang, X. Wang, S. Hu, Z. Qian, R. Han, Dynamic Beat-to-Beat Measurements Of Blood Pressure Using Multimodal Physiological Signals And A Hybrid CNN–LSTM Model, IEEE Journal of Biomedical and Health Informatics, 29(8), 5438–5451, 2025. https://doi.org/10.1109/JBHI.2025.3548771
6. Y. Jia, Y. Zheng, Z. Wang, Y. Li, Non-Invasive Blood Glucose Based On Dual- Wavelength Transmission PPG Signal, IEEE Sensors Journal, 25(7), 11876–11884, 2025.
7. C. Ma, H. Liu, X. Wang, J. Lin, Y. Chen, KD-Informer: A Cuff-Less Continuous Blood Pressure Waveform Estimation Approach Based On Single Photoplethysmography, IEEE Journal of Biomedical and Health Informatics, 27(5), 2219–2230, 2023. https://doi.org/10.1109/JBHI.2022.3181328
8. H. Wang, Q. Xie, X. Li, Y. Qian, G. Li, Self-Supervised Contrastive Learning For Preprocessing PPG Signals In Blood Pressure Prediction, IEEE Sensors Journal, 24(2), 1637–1648, 2024.

https://doi.org/10.1109/JSEN.2023.3324700
9. J. Kim, S. Bickel, M. Jenkins, Calibration-Free BP Estimation Using Multi-Site PPG And A Wave-Based Transformer, IEEE Transactions on Biomedical Engineering, 70(11), 3305–3316, 2023. https://doi.org/10.1109/TBME.2023.3277805
10. Y. Lee, J. Pan, End-To-End Hybrid CNN–GRU Model For Continuous Blood Pressure Estimation From Photoplethysmography, Biomedical Signal Processing and Control, 83, 104642, 2023. https://doi.org/10.1016/j.bspc.2023.104642
11. A. Schlesinger, B. Smith, C. Jones, Y. Zhang, L. Kim, Multimodal Cuffless Blood Pressure Estimation Using ECG, PPG, And Continuous-Time Transformers, IEEE Journal of Biomedical and Health Informatics, 28(3), 1673–1685, 2024. https://doi.org/10.1109/JBHI.2023.3342205
12. A. Hassan, M. Rafiq, A Deep Temporal Convolutional Network For Robust Blood Pres- sure Estimation In Real-World PPG Signals, Computers in Biology and Medicine, 169, 107832, 2024. https://doi.org/10.1016/j.compbiomed.2023.107832
13. W. Cheng, H. Li, D. Zhou, K. Sun, P. Wang, Siamese CNN Models For Personalized Continuous Noninvasive Blood Pressure Estimation, IEEE Access, 11, 150233–150245, 2023. https://doi.org/10.1109/ACCESS.2023.3339
14. F. El-Hajj, P. Kyriacou, K. Budidha, Motion-Artifact-Robust Blood Pressure Estimation Using Adaptive Filtering And Deep Recurrent Networks, IEEE Transactions on Biomedical Engineering, 70(4), 1152–1162, 2023. https://doi.org/10.1109/TBME.2022.3228124
15. N. Liu, Y. Zhao, H. Xu, M. Peng, L. He, A Multi-Scaling Residual Network For Cuff- Less Blood Pressure Estimation Using PPG Signals, Biomedical Signal Processing and Control, 77, 103748, 2022. https://doi.org/10.1016/j.bspc.2022.103748
16. M. Kachuee, M. M. Kiani, H. Mohammadzade, M. Shabany, Cuff-Less Blood Pressure Estimation Algorithms For Continuous Health-Care Monitoring, IEEE Transactions on Biomedical Engineering, 64(4), 859–869, 2017. https://doi.org/10.1109/TBME.2016.2580904
17. G. Slapničar, N. Mlakar, M. Lusˇtrek, Blood Pressure Estimation From Photoplethysmogram Using A Combination Of Handcrafted Features And Deep Learning, Artificial Intelligence in Medicine, 104, 101836, 2019. https://doi.org/10.1016/j.artmed.2020.101836
18. Y. Liang, T. Wu, X. Huang, F. Yu, A New Deep-Learning Model Based On Continuous Wavelet Transform For Cuffless Blood Pressure Estimation, IEEE Sensors Journal, 22(3), 2341–2351, 2022. https://doi.org/10.1109/JSEN.2021.3131235
19. P. Su, R. Xu, L. Ma, Z. Chen, Blood Pressure Estimation Using Photoplethysmography Only: A Deep Learning Approach, IEEE Access, 8, 131790–131801, 2020. https://doi.org/10.1109/ACCESS.2020.3009871
20. M. H. Chowdhury, M. N. I. Shuzan, M. B. I. Reaz, A Lightweight CNN Model For Blood Pressure Estimation Using Fingertip PPG Signals, Computers in Biology and Medicine, 136, 104754, 2021. https://doi.org/10.1016/j.compbiomed.2021.104754
21. Q. Zhang, Z. Zhou, H. Wang, Y. Liang, A Transformer-Based Network For Cuffless Blood Pressure Estimation Using PPG Signals, IEEE Access, 9, 144574–144584, 2021. https://doi.org/10.1109/ACCESS.2021.3122215
22. E. Monte-Moreno, Non-Invasive Estimation Of Blood Glucose And Blood Pressure From A Photoplethysmograph By Means Of Machine-Learning Techniques, Artificial Intelligence in Medicine, 53(2), 127–138, 2011. https://doi.org/10.1016/j.artmed.2011.06.002

23. X. Xing, M. Sun, Optical Blood Pressure Estimation With Photoplethysmography And FFT-Based Filtering, IEEE Sensors Journal, 16(3), 4621–4628, 2016. https://doi.org/10.1109/JSEN.2016.2523861
24. Y. Kurylyak, F. Lamonaca, D. Grimaldi, A Neural Network-Based Method For Continuous Blood Pressure Estimation From PPG Signal, IEEE I2MTC, 280–283, 2013. https://doi.org/10.1109/I2MTC.2013.6555420
25. S. S. Mousavi, M. Firouzmand, D. Fattahi, Blood Pressure Estimation Using CNN–LSTM Architecture From Fingertip PPG Signals, Biomedical Signal Processing and Control, 66, 102458, 2021. https://doi.org/10.1016/j.bspc.2021.102458
26. X. Fan, R. Lin, J. Wang, Y. Du, Multilevel Feature Fusion For Cuffless Blood Pressure Estimation Based On Photoplethysmography, Sensors, 19(24), 5462, 2019. https://doi.org/10.3390/s19245462
27. Y. Sun, J. Zhang, T. Li, X. Xu, Motion-Compensated PPG For Continuous Cuffless Blood Pressure Monitoring, Biomedical Optics Express, 7(8), 3098–3112, 2016. https://doi.org/10.1364/BOE.7.003098
28. H. Shin, Y. Lee, K. Park, Effects Of Aging On PPG Morphology And Blood Pressure Estimation, Journal of Medical Systems, 33(4), 295–301, 2009. https://doi.org/10.1007/s10916-008-9181-2